Electronic Supplementary Information:

Coarse-grained Simulations of Conformational Changes in Multidrug Efflux Transporter AcrB

Yead Jewel, Jin Liu* and Prashanta Dutta*

School of Mechanical and Materials Engineering

Washington State University, Pullman, WA 99164

*Email: jin.liu2@wsu.edu; prashanta@wsu.edu
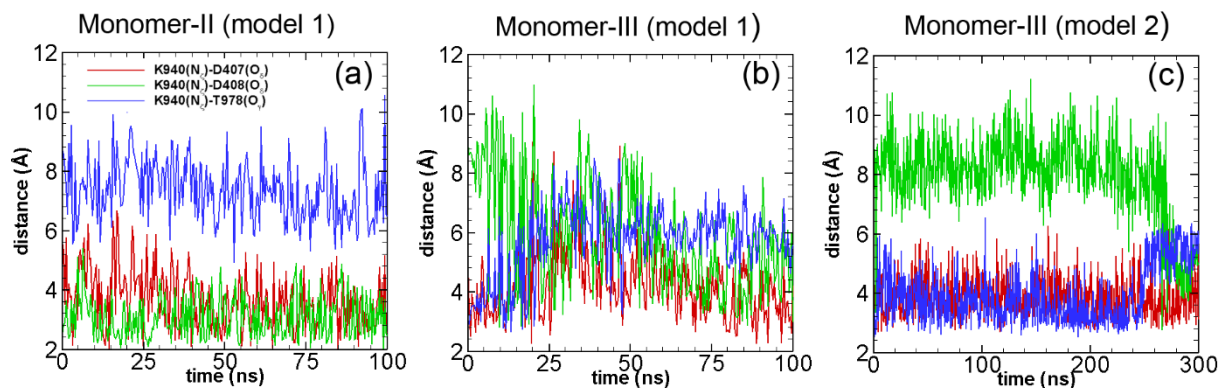
Supplementary Figures:

Figure S1. The side chain dynamics at the TM domain from the second realization. Time evolution of K940-D407 (red), K940-D408 (green) and K940-T978 (blue) distances for monomer II (model 1) **(a)**, monomer III (model 1) **(b)** and monomer III (model 2)**(c)**.
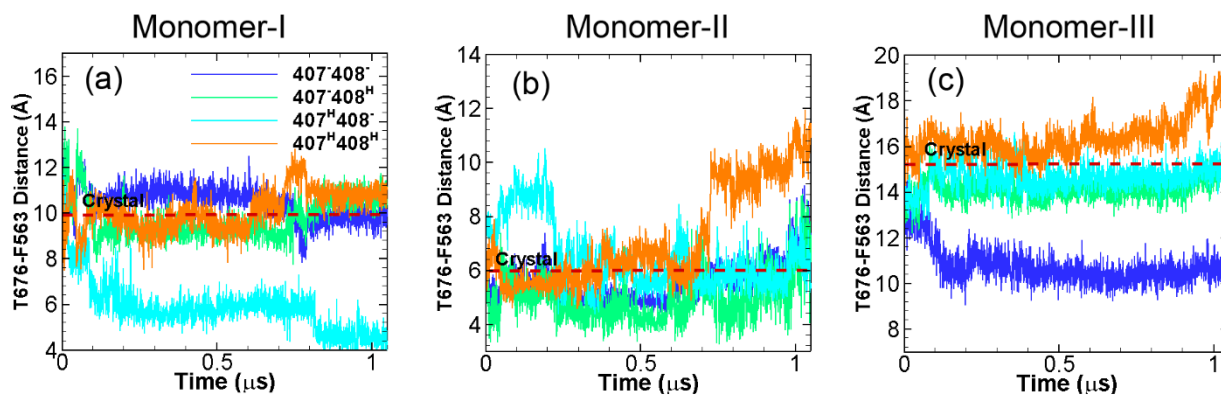

Figure S2. Cleft entrance from the second realization. The time evolution of the T676-F563 distances in monomer I **(a)**, monomer II **(b)** and monomer II **(c)** for the four model systems listed in Table 1.
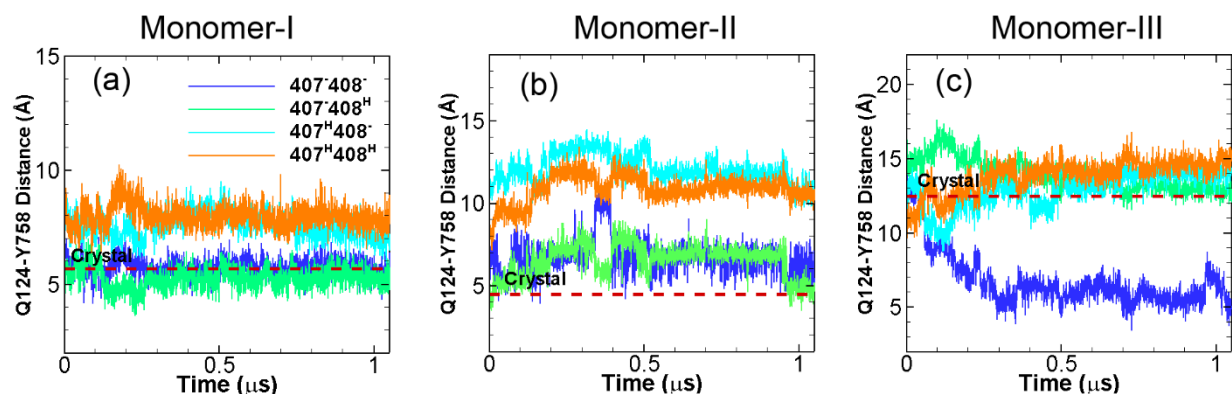
Figure S3. Exit channel from the second realization. The time evolution of the Q124-Y758 distances in monomer I **(a)**, monomer II **(b)** and monomer II **(c)** for the four model systems listed in Table 1.
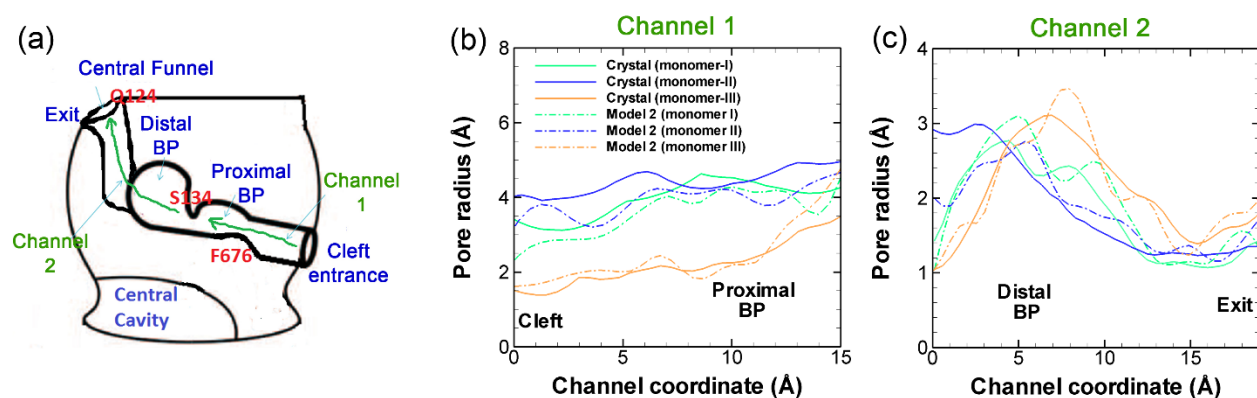

Figure S4. Pore radius profiles. **(a)** Schematic illustration of the substrate transport channel, from the cleft entrance to proximal binding pocket, and then to the distal binding pocket and finally to the exit central funnel exit. The pore radius profiles from the cleft entrance to proximal binding pocket **(b)** and from the distal binding pocket to the exit **(c)** for all three monomers of the model system 2 at the end of the simulation/ The pore radius profiles from the original crystal structure (PDB ID: 2DHH) are also included as solid lines for comparison. The channel 1 coordinate is defined from the cleft to S134, and the channel 2 coordinate is defined from the S134 to the exit.
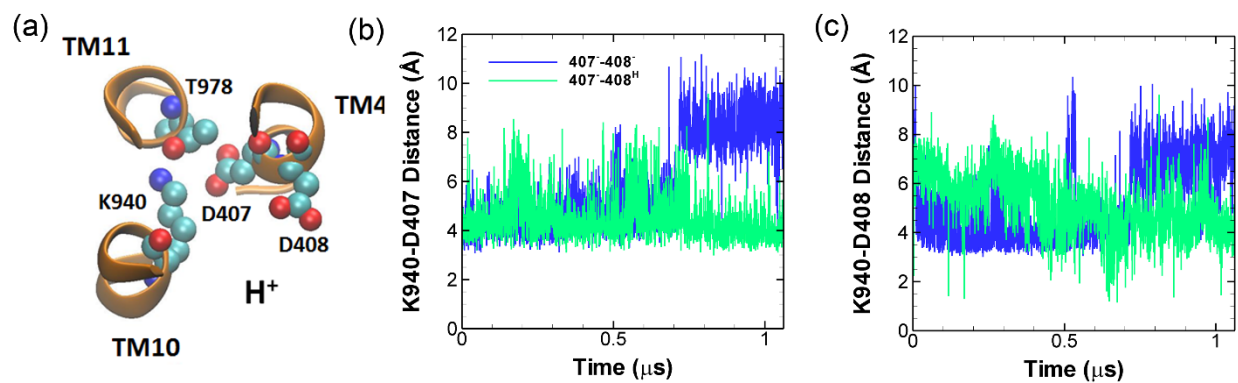
3

Figure S5. (a) Ball and stick representation of the key residues in TM domain. Time evolution of the K940-D407 **(b)** and K940-D408 **(c)** for model system 1 (blue) and model system 2 (green).